TELKOMNIKA Telecommunication, Computing, Electronics and Control
Vol. 19, No. 5, October 2021, pp. 1665~1672
ISSN: 1693-6930, accredited First Grade by Kemenristekdikti, Decree No: 21/E/KPT/2018
DOI: 10.12928/TELKOMNIKA.v19i5.15024

The application of $Ca_5B_2SiO_{10}:Eu^{3+}$ and $YAl_3B_4O_{12}:Ce^{3+},Mn^{2+}$ in dual-layer remote phosphor to enhance lumen output and color quality of WLEDs

Phan Xuan Le, Le Hung Tien
Faculty of Engineering, Van Lang University, Ho Chi Minh City, Viet Nam

Article Info

Article history:

Received Dec 19, 2019
Revised Jul 18, 2021
Accepted Aug 5, 2021

Keywords:

$Ca_5B_2SiO_{10}:Eu^{3+}$
Color quality
Lumen output
Mie-scattering theory
WLEDs
$YAl_3B_4O_{12}:Ce^{3+},Mn^{2+}$

ABSTRACT

This study proposes a dual-layer remote phosphor structure, comprised of a green or a red phosphor layer and a yellow YAG:Ce^{3+} phosphor layer, to enhance color rendering index (CRI) and color quality scale (CQS) of white light-emitting diodes (WLEDs). The phosphors used in this study are green phosphor $YAl_3B_4O_{12}:Ce^{3+},Mn^{2+}$ and red phosphor $Ca_5B_2SiO_{10}:Eu^{3+}$. Besides, the applied WLED structure has the color temperature of 8500 K. The study demonstrates the idea of placing a green phosphor $YAl_3B_4O_{12}:Ce^{3+},Mn^{2+}$ or a red $Ca_5B_2SiO_{10}:Eu^{3+}$ phosphor layer on the yellow phosphor YAG:Ce^{3+} one. After that, the suitable concentration of $Ca_5B_2SiO_{10}:Eu^{3+}$ resulting in the highest color quality is determined. The obtained results showed that $Ca_5B_2SiO_{10}:Eu^{3+}$ is advantageous to CRI and CQS. Particularly, the values of CRI and CQS increased following the growth of $Ca_5B_2SiO_{10}:Eu^{3+}$ concentration, due to the rise in red light components inside WLED's packages. Meanwhile, the luminous flux is benefited by the added green $YAl_3B_4O_{12}:Ce^{3+},Mn^{2+}$ phosphor. However, there are decreases in lumen output and color quality when the concentrations of $Ca_5B_2SiO_{10}:Eu^{3+}$ and $YAl_3B_4O_{12}:Ce^{3+},Mn^{2+}$ rise over the corresponding levels. This result is proved via using Mie-scattering theory and Lambert-Beer's law. In short, the findings of the research paper are valuable references for high-light-quality WLEDs fabrication.

Corresponding Author:

Phan Xuan Le
Faculty of Engineering
Van Lang University
No. 45 Nguyen Khac Nhu Street, Ho Chi Minh City, Vietnam
Email: le.px@vlu.edu.vn

1. INTRODUCTION

These days, the conventional light source is not able to meet the requirements of modern applications. Thus, the fourth-generation light source called phosphor-converted white light-emitting diodes (pc-WLEDs) is used as an alternative which can bring better prospects in lighting solutions [1]. Its applications have spread out in many different aspects of human life, including landscape, street lighting, and backlighting. However, white light-emitting diodes (LEDs') development is still restricted due to the inefficient light extraction and inhomogeneous angular-dependent correlated color temperature [2]. Therefore, to be able to meet the rising demand of the illumination market, it is essential to make further breakthroughs in luminous efficiency and color quality [3]. Nowadays, the most popular approach to generate white light is to combine yellow lights converted by red phosphors with blue lights emitted from LED chip.

In addition, how phosphor layers in the LED package are arranged plays an important role that affects the luminous efficiency, especially the color rendering index [4]-[8]. There have been many common phosphor coating methods applied for LEDs' production including dispensing coating and conformal coating [9], [10]. However, the color quality provided by these structures is not high. The cause is that the light conversion of phosphor material degrades due to the direct contact of yellow light-emitting phosphor with the LED chip that causes the temperature at their interface to increase. Thus, a heat reduction at that junction is essential and potential to enhance the performance of phosphors and prevent them from the irreversible destruction. In various studies, the remote phosphor structure is confirmed to have the ability of reducing the heat effect because the phosphor layer is separated far from the LED chip-heat source. Specifically, an appropriate distance between the phosphor layer and the LED chip could create a limitation in the backscattering and circulation of light inside the LEDs. Therefore, we can control the heat of LED by applying this method, and then improve luminous output and white-light chromaticity of LEDs [11]-[16]. Though in terms of regular lighting, this remote phosphor structure is an optimal solution, it cannot completely fulfill the specifications of many other illumination applications, leading to a need of fabricating the next generation of LED. To accomplish that purpose, there are several advanced remote phosphor structures proposed to reduce the light scattering backward to the chip and improve the luminous efficacy. The light from the LED chip can be redirected to the LED's surface by using an inverted cone lens encapsulant combining with a surrounding ring remote phosphor layer. Moreover, they can reduce the light loss inside LED which occurs due to the internal reflection [17]. Besides, as mentioned in another study, high angular correlated color temperature uniformity and better color stability can be achieved with a patterned remote phosphor configuration having a clear zone in the perimeter area that is not coated by phosphor on the surrounding surface [18]. Additionally, in a far field pattern, the patterned sapphire substrate used in the remote phosphor structure can bring much higher correlated color temperature homogeneity than in a conventional pattern [19]-[22]. Then, the dual-layer remote phosphor is proposed to accomplish the improvement of the light output of LEDs. Previous studies working on this focused on the enhancement of color homogeneity and lumen output of WLEDs built with dual-layer remote phosphor structure. However, the WLED packages studied in these research papers use single LED chip and have low color temperatures, which means their results are not practical when applying for the WLEDs with high color temperature because of the complication in improving their optical parameters. In addition to that, the comparison among the results of using different dual-layer phosphor configurations has not been mentioned in any study before. Thus, manufacturers may face many obstacles in selecting a suitable structure to improve the color quality or luminous efficiency of their WLED products.

Acknowledging the difficulties, this article will propose two different dual-layer remote phosphor structures to enhance the color quality and lumen efficacy of WLEDs having high color temperature at 8500 K. The paper uses two kinds of phosphor layer to achieve the goal, one is the green phosphor layer of $YAl_3B_4O_{12}:Ce^{3+},Mn^{2+}$ and the other is the red $Ca_5B_2SiO_{10}:Eu^{3+}$ phosphor layer. The purpose of using the green phosphor $YAl_3B_4O_{12}:Ce^{3+},Mn^{2+}$ is to increase the green light component in WLEDs to increase luminous flux, while the red $Ca_5B_2SiO_{10}:Eu^{3+}$ phosphor will help to rise the red light component and then increase color rendering index (CRI) and color quality scale (CQS) as a result. In addition, the article includes a detail chemical composition of $Ca_5B_2SiO_{10}:Eu^{3+}$ and $YAl_3B_4O_{12}:Ce^{3+},Mn^{2+}$ as well as a specific comparison between the effects on the optical properties of WLEDs between these two remote phosphor layer structures. From the results demonstrated in the paper, both CRI and CQS show an improvement with the addition of phosphor $Ca_5B_2SiO_{10}:Eu^{3+}$. However, there is a sharp decrease in the white-light chromaticity and luminescence efficiency of WLEDs when the concentrations of $YAl_3B_4O_{12}:Ce^{3+},Mn^{2+}$ and $Ca_5B_2SiO_{10}:Eu^{3+}$ exceed the limit amount. Therefore, it is important to determine appropriate concentrations of these two phosphors to avoid that significant reduction. Besides, there are two differences we can conclude from the results of the research with the presence of the red or green phosphor layer above the yellow phosphor layer of YAG:Ce^{3+} in the package. First, the increase of the blue or red light component contributes to the growth of the spectrum of white light, which is the main factor determining the enhancement of the color homogeneity. Second, the scattering and transmission of lights in WLEDs are not compatible with the concentration of added phosphors. In other words, these light properties are in inverse proportion to the trends of phosphor concentrations. Thus, to get the better lumen efficacy of WLEDs, finding an appropriate value of phosphor concentration is also another crucial part of this research.

2. PREPARATION

The red $Ca_5B_2SiO_{10}:Eu^{3+}$ and green $YAl_3B_4O_{12}:Ce^{3+},Mn^{2+}$ phosphor compositions are indispensable parts of this research. So, in order to have the best phosphor layers that can give the exact results, we need to have the phosphor material well-prepared. The composition of red $Ca_5B_2SiO_{10}:Eu^{3+}$ phosphor includes 4 different ingredients, as listed in Table 1. The process to get this red phosphor is a 3-stage-firing process.

Before starting the first stage, all the ingredients must be mix by dry milling or grinding to create a homogeneous mixture. Then, fire this mixture in open quartz boats at 1100 ^{0}C for an hour. After 1 hour is over, take this mixture out and powderize it by using the milling method. Next is the second stage of firing. The powderized product is fired again in open quartz boats within 1 hour and at the temperature of 1200 ^{0}C. When this stage finishes, the material will go through another powderizing step. After that, the third firing stage will be conducted in the same container and time as the two previous ones, but the firing temperature for this time is set at 1300 ^{0}C.

For green $YAl_3B_4O_{12}:Ce^{3+},Mn^{2+}$ phosphor composition, its ingredients is more than that of red $Ca_5B_2SiO_{10}:Eu^{3+}$, and they are detailed in Table 2. The preparation process of this green phosphor composition consists of 4 stages of firing and powderizing. The firing time for those stages is within 1 hour, and the powderizing process occurs right after each firing finishes. Initially, it is essential to mix the chemical elements together by dry grinding or milling. Then, the process of firing and powderizing will start. For the first time, the mixture will be fired in open quartz boats at about 500 ^{0}C. In the next 3 stages, the firing will occur in open alumina crucibles, but at different temperatures and with different airflows. In the second firing, the flow of N2 will be added and fired with the material at 900 ^{0}C. The third firing will be carried out with the addition of CO airflow and the temperature of 1100 ^{0}C. Finally, for the fourth stage, the material will be fired with CO at 1200 ^{0}C. After the fourth powderizing finishes, the attain product will be washed in hot water several times and then dried to get the required green $YAl_3B_4O_{12}:Ce^{3+},Mn^{2+}$ phosphor. Two models of WLED used in experiments are green-yellow dual-layer remote phosphor configuration (GYC) and red-yellow dual-layer remote phosphor configuration (RYC). In both configurations, the phosphor layers are placed above blue LED chips. For GYC structure, the green phosphor layer $YAl_3B_4O_{12}:Ce^{3+},Mn^{2+}$ is on the $YAG:Ce^{3+}$ yellow one, as presented in Figure 1 (a). Meanwhile, in RYC structure, with the red phosphorus film is arranged above the yellow $YAG:Ce^{3+}$ layer is the layer of red phosphor $Ca_5B_2SiO_{10}:Eu^{3+}$, showed in Figure 1 (b). As mentioned in the previous part, the purpose of applying GYC and RYC structures is to have the color and optical quality of WLEDs enhanced by increasing the green and red light components, as well as their scattering inside the WLED packages. Simultaneously, the concentrations of $YAl_3B_4O_{12}:Ce^{3+},Mn^{2+}$ and $Ca_5B_2SiO_{10}:Eu^{3+}$ phosphor need to be adjusted.

Table 1. Composition of red-emitting $Ca_5B_2SiO_{10}:Eu^{3+}$ phosphor

Ingredients	Mole %	By weight (g)
$CaCO_3$	100	100
H_2BO_3	50	31
SiO_2	22	13.2
Eu_2O_3	5 (of Eu)	8.8

Table 2. Composition of green-emitting $YAl_3B_4O_{12}:Ce^{3+},Mn^{2+}$ phosphor

Ingredients	Mole %	By weight (g)
Y_2O_3	80 (of Y)	90.4
CeO_2	10	17.2
Tb_4O_7	10 (of Tb)	18.7
Al_2O_3	300 (of Al)	153
H_3BO_3	410	254

(a) (b)

Figure 1. Illustration of: (a) GYC and (b) RYC

The two charts of Figure 2 show that the changes of both green $YAl_3B_4O_{12}:Ce^{3+},Mn^{2+}$ and red $Ca_5B_2SiO_{10}:Eu^{3+}$ phosphor concentrations are in an opposite trend with that of the yellow $YAG:Ce^{3+}$ phosphor. This change has two functions: keeping the average correlated color temperatures (ACCTs) stable and affecting the scattering and absorption properties of phosphor layers in WLEDs, which probably influences the color performance and lumen output of WLEDs. Therefore, it can be said that the choice of the concentrations of $YAl_3B_4O_{12}:Ce^{3+},Mn^{2+}$ and $Ca_5B_2SiO_{10}:Eu^{3+}$ phosphor is a decisive factor to the color quality of WLEDs. According to the illustrations of Figure 2, as the concentration of $YAl_3B_4O_{12}:Ce^{3+},Mn^{2+}$ and $Ca_5B_2SiO_{10}:Eu^{3+}$ increase from 2 to 20% wt., the $YAG:Ce^{3+}$ concentration decreases in order to maintain the ACCTs. Moreover, for the WLEDs having high color temperature of 8500 K, this opposite change also occurs, similar to the ones with lower ACCTs.

Next, the significant influence of red phosphor $Ca_5B_2SiO_{10}:Eu^{3+}$ over the spectrum of WLEDs is demonstrated clearly in Figure 3. For the WLEDs requiring high color quality, it is acceptable to reduce a small amount of luminous flux. Before demonstrating the impact of $Ca_5B_2SiO_{10}:Eu^{3+}$, it is necessary to take a look at how $YAl_3B_4O_{12}:Ce^{3+},Mn^{2+}$ phosphor affect the emission spectrum of WLEDs. Obviously, the spectral intensity in 420-480 nm and 500-640 nm wavelength ranges increases with the presence of $YAl_3B_4O_{12}:Ce^{3+},Mn^{2+}$, which means the luminous flux is also improved. From this result, the blue-light scattering of the WLED also increases, indicating that there is more phosphor scattering events occur inside WLEDs, and benefiting the copper color as a result. This result shows the importance of the green phosphor $YAl_3B_4O_{12}:Ce^{3+},Mn^{2+}$ application to enhance the WLEDs' optical properties. In terms of using $Ca_5B_2SiO_{10}:Eu^{3+}$ phosphor, it is easy to realize the upward trend of the LEDs' spectrum in the same two spectral regions as those of the $YAl_3B_4O_{12}:Ce^{3+},Mn^{2+}$, 420-480 nm and 500-640 nm. Moreover, with the addition of this red phosphor, the red light spectrum also increases in the 648-738 nm wavelength band. However, if there is no spectral increase in the two previous wavelength bands, this increase is not noticeable because when the spectrum increases in 420-480 nm and regions 500-640 nm help to improve the luminous flux of blue light (blue-light scattering). Furthermore, it is obvious that in the mentioned spectral regions, the higher the color temperature is, the better the emission spectrum becomes. This means higher color temperature results in better color and optical quality. Therefore, the study can assure that $Ca_5B_2SiO_{10}:Eu^{3+}$ is the right choice in improving the color quality of high-color-temperature WLEDs (8500 K). This achieved result of $Ca_5B_2SiO_{10}:Eu^{3+}$ application is important to manufacturers, especially while keeping the quality of WLEDs having high color temperature under control still confronts many obstacles. Finally, based on what the manufacturers require, the final dual-layer remote phosphor structure can be decided.

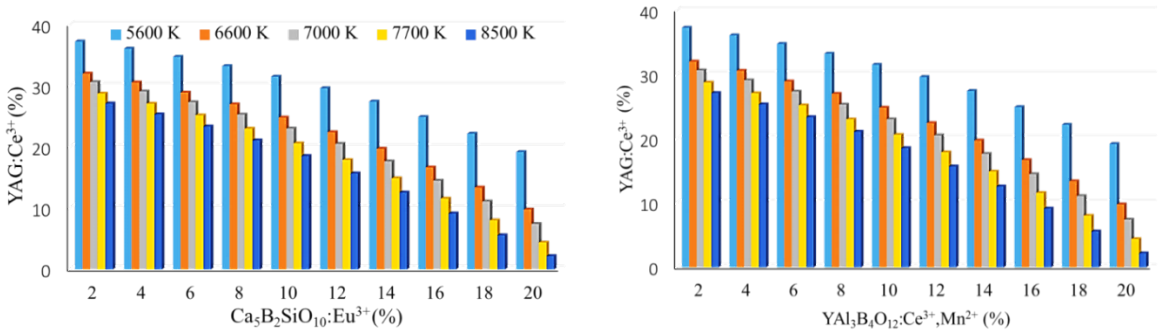

Figure 2. The change of phosphor concentration of: (a) RYC and (b) GYC for keeping the average CCT

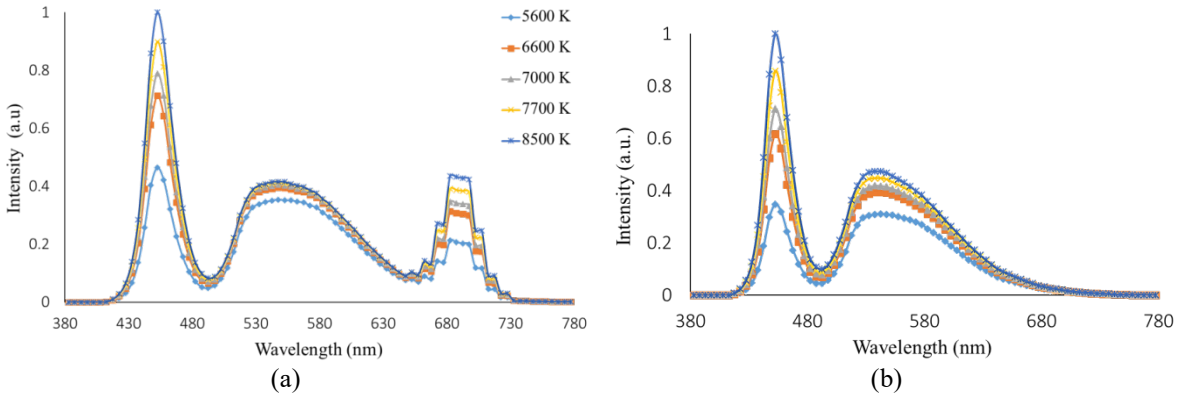

Figure 3. Emission spectra of: (a) RYC and (b) GYC

3. RESULTS AND DISCUSSION

The CRI is a measurement of the ability of the light source in showing the true color of the object they illuminated. The color imbalance occurs among the three primary colors: red, yellow, and blue when the green light components increase more than the two other ones. This imbalance will cause a disadvantage to the color quality of WLEDs and then get the color integrity of WLEDs reduced. With the addition of

$YAl_3B_4O_{12}:Ce^{3+},Mn^{2+}$, there is a small decrease in CRI, as shown in Figure 4. However, this reduction is acceptable, as CRI is just a part of CQS. CQS is a synthetic index the three crucial factors: CRI, viewers' preference, and the color coordinate. Thus, CQS is considered as a more overall measurement in color quality evaluation. This also explains why CQS is much more complicated and challenging to accomplish than CRI. Figure 5 shows the change of CQS in connection with different amounts of $YAl_3B_4O_{12}:Ce^{3+},Mn^{2+}$ concentration. With the concentration of $YAl_3B_4O_{12}:Ce^{3+},Mn^{2+}$ concentration less than 8%, the CQS is stable. However, if the concentration of $YAl_3B_4O_{12}:Ce^{3+},Mn^{2+}$ continues to increase from 8%, CQS starts to decreases, and the sharp decline occurs when the concentration is from 12 to 20%. Thus, 8% $YAl_3B_4O_{12}:Ce^{3+},Mn^{2+}$ is a suitable concentration for maintaining the high CQS of LEDs, after weighing up the reduction of emitted luminous flux.

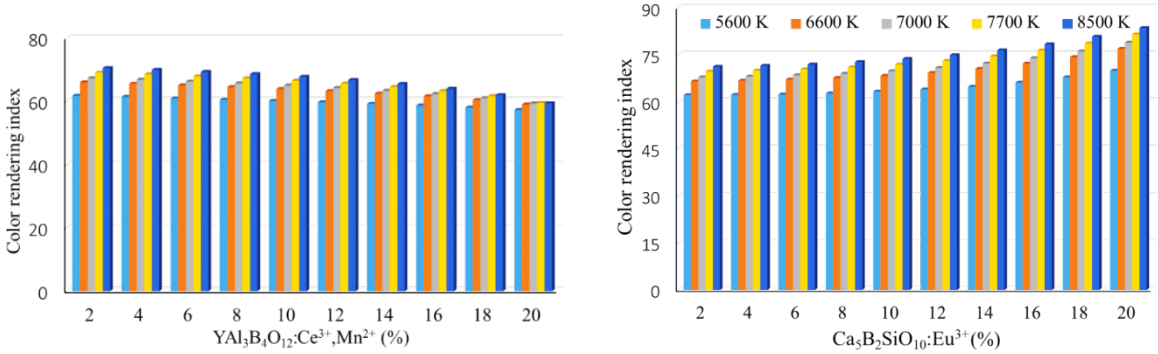

Figure 4. The color rendering index as a function of the concentration of:
(a) $YAl_3B_4O_{12}:Ce^{3+},Mn^{2+}$ and (b) $Ca_5B_2SiO_{10}:Eu^{3+}$

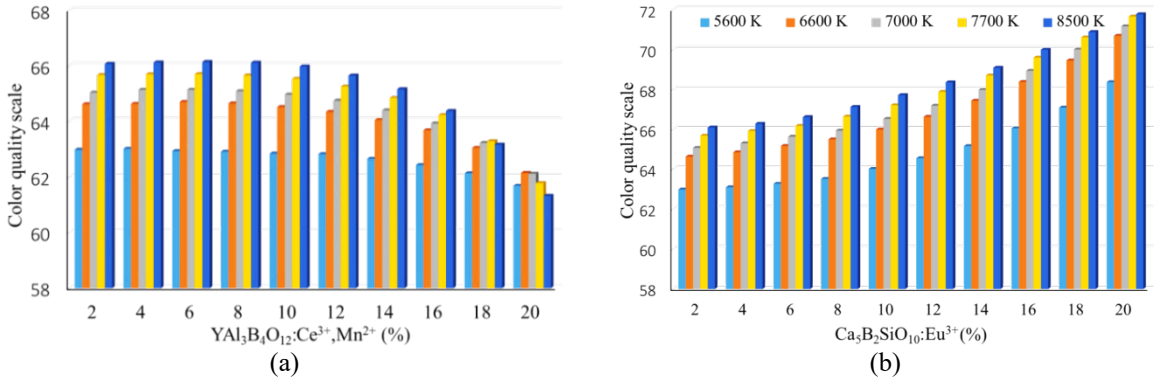

Figure 5. The color quality scale as a function of the concentration of:
(a) $YAl_3B_4O_{12}:Ce^{3+},Mn^{2+}$ and (b) $Ca_5B_2SiO_{10}:Eu^{3+}$

Different from the results when using $YAl_3B_4O_{12}:Ce^{3+},Mn^{2+}$, CRI values increase with the growth of $Ca_5B_2SiO_{10}:Eu^{3+}$ concentration, as can be seen in Figure 4. The absorption characteristic of the red phosphor layer is the force behind this better CRI. In specific, as soon as the phosphor $Ca_5B_2SiO_{10}:Eu^{3+}$ absorbs blue light from LED chip, it turns blue light into red light. Moreover, this red $Ca_5B_2SiO_{10}:Eu^{3+}$ also absorbs yellow light inside the LEDs. However, the blue-light absorption is stronger than the yellow-light one, leading to the increase in red light components in WLEDs. As a result, CRI is lifted up. It is obvious that CRI is an important parameter for a good modern LED lamp. Thus, it is easy to understand that the higher the CRI of a LED, the higher the price of it becomes. In addition to the ability of enhancing the CRI, the other benefit of using $Ca_5B_2SiO_{10}:Eu^{3+}$ is low cost, which contributes to spreading its application in LED production. However, it is impossible to conclude that a LED can generate good color quality if it has a high CRI index. As mentioned in the above paragraph, CRI is included in CQS, and thus CQS is the main goal of recent researches when it comes to bettering the color quality of LEDs. With the application of $Ca_5B_2SiO_{10}:Eu^{3+}$, it is possible to increase the CQS, from which the enhancement of color quality can be accomplished. As

shown in Figure 5, CQS values rise up significantly in accordance with the increase of $Ca_5B_2SiO_{10}:Eu^{3+}$ concentration. The disadvantage in lumen output of $Ca_5B_2SiO_{10}:Eu^{3+}$, however, cannot be ignored.

In this part, the converted yellow light and the transmitted blue light in the dual-layer remote phosphor structure are calculated using a series of mathematic expressions, demonstrated below. From this demonstration, we can make a huge development in LED efficiency.

The two following formulas express the transmitted blue light and converted yellow light in a single- layer remote phosphor package having *2h* phosphor-layer thickness:

$$PB_1 = PB_0 \times e^{-2\alpha_{B1}h} \quad (1)$$

$$PY_1 = \frac{1}{2}\frac{\beta_1 \times PB_0}{\alpha_{B1}-\alpha_{Y1}}(e^{-2\alpha_{Y1}h} - e^{-2\alpha_{B1}h}) \quad (2)$$

For the dual-layer configuration, the transmitted blue light and converted yellow light are defined via the next two expressions, given that each phosphor layer thickness is *h*:

$$PB_2 = PB_0 \times e^{-2\alpha_{B2}h} \quad (3)$$

$$PY_2 = \frac{1}{2}\frac{\beta_2 \times PB_0}{\alpha_{B2}-\alpha_{Y2}}(e^{-2\alpha_{Y2}h} - e^{-2\alpha_{B2}h}) \quad (4)$$

In these expressions, the single-layer and dual-layer remote phosphor models are expressed by the subscripts "*1*" and "*2*", respectively. *h* indicates each phosphor layer thickness. β is the conversion coefficient for blue light converting to yellow light while γ indicates the reflection coefficient of the yellow light. PB_0 presents the light intensity from blue LED which includes the intensities of blue light (*PB*) and yellow light (*PY*). α_B and α_Y characterize the fractions of the energy loss of blue and yellow lights during their multiplication in the phosphor layer separately.

The significant enhancement of the lighting performance of dual-layer phosphor WLEDs, by comparison with that of the single-layer phosphor WLED, can be expressed as (5).

$$\frac{(PB_2+PY_2)-(PB_1+PY_1)}{PB_1+PY_1} > 0 \quad (5)$$

Based on Mie-theory [23], [24], the scattering of the phosphor particles was determined, and the scattering cross section C_{sca} for spherical particles can be computed. Moreover, the Lambert-Beer law [25], [26] is applied to measure the transmitted light power.

$$I = I_0 exp(-\mu_{ext} L) \quad (6)$$

In which, I_0 indicates the incident light power, *L* represents for the phosphor layer thickness (*mm*) and μ_{ext} is the extinction coefficient that can be expressed as: $\mu_{ext} = N_r.C_{ext}$, where N_r is the number density distribution of particles (mm^{-3}) and C_{ext} (mm^2) is the extinction cross-section of phosphor particles.

As can be seen from (5), WLEDs with dual-layer phosphor configuration provides better luminescence performance than single-layer phosphor one. Hence, the efficiency of the dual-layer remote phosphor in improving the luminous flux of LEDs is proved in this research paper. Additionally, changes of luminous flux with the concentrations of $YAl_3B_4O_{12}:Ce^{3+},Mn^{2+}$ and $Ca_5B_2SiO_{10}:Eu^{3+}$ phosphors are shown in Figure 6. Apparently, with the rise of $YAl_3B_4O_{12}:Ce^{3+},Mn^{2+}$ concentration from 2 to 20% wt, the luminous flux is better. Meanwhile, a sharp decline occurs to the luminous flux when there is an increase of the $Ca_5B_2SiO_{10}:Eu^{3+}$ concentration. This case can be explained by applying the Beer's law, in which the reduction factor μ_{ext} is in direct proportion to the concentration of $Ca_5B_2SiO_{10}:Eu^{3+}$ but in inverse proportion to the transmission energy of lights. If both phosphor layer thicknesses in WLEDs are constant parameters, the lumen output may show a downward trend when the concentration of $Ca_5B_2SiO_{10}:Eu^{3+}$ increases. From the above chart of Figure 6, at the $Ca_5B_2SiO_{10}:Eu^{3+}$ concentration of 20% wt., the luminous flux reaches the lowest values. Nevertheless, the red phosphor layer $Ca_5B_2SiO_{10}:Eu^{3+}$ is beneficial to the CRI and CQS of LEDs, and the luminous output of RYC dual-layer phosphor structure is also better than that of the single-layer phosphor one (not using the red phosphor layer). Thus, after considering these benefits, the decrease of luminous flux cause by $Ca_5B_2SiO_{10}:Eu^{3+}$ is allowable. The last concern is the manufacturers' goal, based on which an appropriate concentration $Ca_5B_2SiO_{10}:Eu^{3+}$ is decided to apply in the mass-production of LEDs.

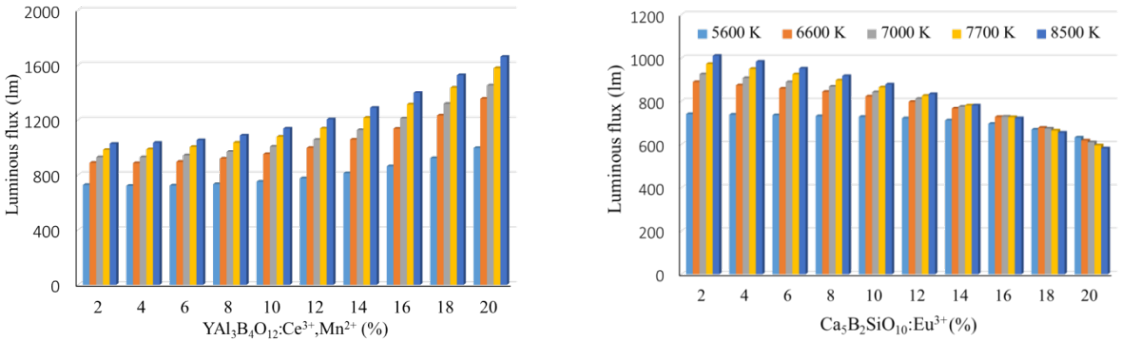

Figure 6. The lumen output as a function of the concentration of;
(a) $YAl_3B_4O_{12}:Ce^{3+},Mn^{2+}$ and (b) $Ca_5B_2SiO_{10}:Eu^{3+}$

4. CONCLUSION

The influences of green $YAl_3B_4O_{12}:Ce^{3+},Mn^{2+}$ red $Ca_5B_2SiO_{10}:Eu^{3+}$ phosphors on CRI, CQS and lumen efficiency of dual-layer phosphor structures are demonstrated in this study. By applying the Mie-scattering theory and the Lambert-Beer law, the paper has examined the attained experimental results and drawn a conclusion that $Ca_5B_2SiO_{10}:Eu^{3+}$ is the right selection for achieving the enhancement in color quality of WLEDs. Besides, if the goal is to improve the lumen efficacy of LEDs, the green $YAl_3B_4O_{12}:Ce^{3+},Mn^{2+}$ phosphor is a better option than the other one. The results are both true with the WLEDs having low and high or even higher 8500 K color temperatures. Therefore, the findings in this article have accomplished the difficult target that the remote phosphor structure have been facing: promoting better the color quality for WLEDs. However, there are existing disadvantages to the luminous flux or color quality of WLEDs when using these phosphor layers. Specifically, with a large increase in the concentrations of $YAl_3B_4O_{12}:Ce^{3+},Mn^{2+}$ or $Ca_5B_2SiO_{10}:Eu^{3+}$, the color quality or luminous flux shows a significant decrease. Hence, an appropriate of these phosphor concentrations is very important to the optical performance of WLEDs, based on the requirements of manufacturers. With these findings, this study can become a great reference for manufacturing better WLED generations.

REFERENCES

[1] J. Chen, B. Fritz, G. Liang, X. Ding, U. Lemmer, and G. Gomard, "Microlens arrays with adjustable aspect ratio fabricated by electrowetting and their application to correlated color temperature tunable light-emitting diodes," *Optics Express,* vol. 27, no. 4, pp. A25-A38, 2019, doi: 10.1364/OE.27.000A25.
[2] C. McDonnell, E. Coyne, and G. M. O'Connor, "Grey-scale silicon diffractive optics for selective laser ablation of thin conductive films," *Applied Optics,* vol. 57, no. 24, pp. 6966-6970, 2018, doi: 10.1364/AO.57.006966.
[3] A. D. Corbett *et al.*, "Microscope calibration using laser written fluorescence," *Opt. Express,* vol. 26, no. 17, pp. 21887-21899, 2018, doi: 10.1364/OE.26.021887.
[4] K. Orzechowski, *et al.*, "Optical properties of cubic blue phase liquid crystal in photonic microstructures," *Opt. Express,* vol. 27, no. 10, pp. 14270-14282, 2019, doi: 10.1364/OE.27.014270.
[5] S. J. Dain, D. A. Atchison, J. K. Hovis, M.-Y. Boon, "Lighting for color vision examination in the era of LEDs: the FM100Hue Test," J. *Opt. Soc. Am. A,* vol. 37, no. 4, pp. A122-A132, 2020, doi: 10.1364/JOSAA.382301.
[6] T. Hu *et al.*, "Demonstration of color display metasurfaces via immersion lithography on a 12-inch silicon wafer," *Opt. Express,* vol. 26, no. 15, pp. 19548-19554, 2018, doi: 10.1364/OE.26.019548.
[7] J. Ruschel *et al.*, "Current-induced degradation and lifetime prediction of 310 nm ultraviolet light-emitting diodes," *Photon. Res*, vol. 7, no. 7, pp. B36-B40, 2019, doi: 10.1364/PRJ.7.000B36.
[8] A. A. Kaminari, S. Boyatzis, and A. Alexopoulou, "Linking Infrared Spectra of Laboratory Iron Gall Inks Based on Traditional Recipes with their Material Components," *Appl. Spectros,* vol. 72, no. 10, pp. 1511-1527, 2018, doi: 10.1177/0003702818778319.
[9] M. E. Kandel, W. Lu, J. Liang, O. Aydin, T. A. Saif, and G. Popescu, "Cell-to-cell influence on growth in large populations," *Biomed. Opt. Express,* vol. 10, no. 9, pp. 4664-4675, 2019, doi: 10.1364/BOE.10.004664.
[10] R. A. Deshpande, A. S. Roberts, and S. I. Bozhevolnyi, "Plasmonic color printing based on third-order gap surface plasmons [Invited]," *Opt. Mater. Express,* vol. 9, no, 2, pp. 717-730, 2019, doi: 10.1364/OME.9.000717.
[11] Y. Zhang, J. Wang, W. Zhang, S. Chen, and L. Chen, "LED-based visible light communication for color image and audio transmission utilizing orbital angular momentum superposition modes," *Opt. Express,* vol. 26, no. 13, pp. 17300-17311, 2018, doi: 10.1364/OE.26.017300.

[12] J. Cao, J. Zhang, and X. Li, "Upconversion luminescence of Ba_3La , $PO_{4.3}$:Yb^{3+}-Er^{3+}/Tm^{3+} phosphors for optimal temperature sensing," *Appl. Opt*, vol. 57, no. 6, pp. 1345-1350, 2018, doi: 10.1364/AO.57.001345.
[13] Z. Li, Y. Tang, J. Li, X. Ding, C. Yan, and B. Yu, "Effect of flip-chip height on the optical performance of conformal white-light-emitting diodes," *Opt. Lett*, vol. 43, no. 5, pp. 1015-1018, 2018, doi: 10.1364/OL.43.001015.
[14] Y. Shi, S. Ye, J. Yu, H. Liao, J. Liu, and D. Wang, "Simultaneous energy transfer from molecular-like silver nanoclusters to Sm^{3+}/Ln^{3+}, Ln = Eu or Tb. in glass under UV excitation," *Opt. Express,* vol. 27, no. 26, pp. 38159-38167, 2019, doi: 10.1364/OE.380860.
[15] G. Xia, Y. Ma, X. Chen, S. Q. Jin, and C. Huang, "Comparison of MAP method with classical methods for bandpass correction of white LED spectra," *J. Opt. Soc. Am. A,* vol. 36, no. 5, pp. 751-758, 2019, doi: 10.1364/JOSAA.36.000751.
[16] S. Kashima *et al.*, "Wide field-of-view crossed Dragone optical system using anamorphic aspherical surfaces," *Appl. Opt*, vol. 57, no. 15, pp. 4171-4179, 2018, doi: 10.1364/AO.57.004171.
[17] M. C. Aguilar *et al.*, "Automated instrument designed to determine visual photosensitivity thresholds," *Biomed. Opt. Express*, vol. 9, no. 11, pp. 5583-5596, 2018, doi: 10.1364/BOE.9.005583.
[18] H. Jia *et al.*, "High-transmission polarization-dependent active plasmonic color filters," *Appl. Opt*, vol. 58, no. 3, pp. 704-711, 2019, doi: 10.1364/AO.58.000704.
[19] N. Bamiedakis *et al.*, "Ultra-Low Cost High-Density Two-Dimensional Visible-Light Optical Interconnects," in *Journal of Lightwave Technology*, vol. 37, no. 13, pp. 3305-3314, 1 July1, 2019, doi: 10.1109/JLT.2019.2914310.
[20] L. Xiao, C. Zhang, P. Zhong, and G. He, "Spectral optimization of phosphor-coated white LED for road lighting based on the mesopic limited luminous efficacy and IES color fidelity index," *Appl. Opt,* vol. 57, pp. 931-936, 2018, doi: 10.1364/AO.57.000931.
[21] H. Y. Yu *et al.*, "Solar spectrum matching with white OLED and monochromatic LEDs," *Appl. Opt,* vol. 57, no. 10, pp. 2659-2666, 2018, doi: 10.1364/AO.57.002659.
[22] T.-C. Bui, R. Cusani, G. Scarano, and M. Biagi, "Metameric MIMO-OOK transmission scheme using multiple RGB LEDs," *Opt. Express,* vol. 26, no. 11, pp. 14038-14050, 2018, doi: 10.1364/OE.26.014038.
[23] X. Huang *et al.*, "Effect of electron-transfer quenching on the photoluminescence of Pr^{3+} in $MgXO_3$, X = Ge,Si," *Opt. Mater. Express*, vol. 10, no. 5, pp. 1163-1168, 2020, doi: 10.1364/OME.389599.
[24] X. Li, D. Kundaliya, Z. J. Tan, M. Anc, and N. X. Fang, "Projection lithography patterned high-resolution quantum dots/thiol-ene photo-polymer pixels for color down conversion," *Opt. Express,* vol. 27, no. 21, pp. 30864-30874, 2019, doi: 10.1364/OE.27.030864.
[25] T. Shang, Z. P. Sun, Z. Y. Dong, and Q. Li, "Network selection method based on MADM and VH-based multi-user access scheme for indoor VLC hybrid networks," *Opt. Express,* vol. 26, no. 23, pp. 30795-30817, 2018, doi: 10.1364/OE.26.030795.
[26] V. Dumont, S. Bernard, C. Reinhardt, A. Kato, M. Ruf, and J. C. Sankey, "Flexure-tuned membrane-at-the-edge optomechanical system," *Opt. Express,* vol. 27, no. 18, pp. 25731-25748, 2019, doi: 10.1364/OE.27.025731.